PROCEEDINGS OF SCIENCE

CMS RPC System status and performance in Run3

Mauricio Thiel[a,*] **on behalf of the CMS Collaboration**

[a] *Departamento de Física Nuclear e Altas Energias (DFNAE), Universidade do Estado do Rio de Janeiro (UERJ), Rua São Francisco Xavier, 524, Maracanã, Rio de Janeiro, Brazil*

E-mail: mauricio.thiel@cern.ch

The Compact Muon Solenoid (CMS) experiment is a multipurpose detector, located at the Large Hadron Collider (LHC) at CERN. It is equipped with several subdetector systems to reconstruct high-energy collision particles. Resistive Plate Chambers (RPC), known for their fast response and good timing resolution, are used as one of the subdetectors for muon detection within the CMS Muon System. RPCs detect ionizing particles through gas avalanches between resistive plates, producing signals on readout strips. During 2024, the CMS experiment recorded over 112 fb^{-1} of proton-proton collision data, bringing the total for Run 3 (2022–present) to more than 250 fb^{-1}. To secure good data quality throughout this period, the performance and stability of the RPC system are continuously monitored, and the latest results will be presented.

PoS(EPS-HEP2025)487

*Speaker

ISSN 1824-8039. Published by SISSA Medialab.

https://pos.sissa.it/

1. The CMS Experiment and Muon System

The Compact Muon Solenoid (CMS) experiment [1] is a general-purpose detector operating at the Large Hadron Collider (LHC) at CERN. It is designed to investigate a wide range of phenomena at the highest energies achieved in a collider. CMS employs several complementary subdetector systems to reconstruct the complex final states of proton-proton collisions with high precision. This versatility allows the experiment to explore both precision measurements of the Standard Model and searches for new physics beyond it.

A central component of CMS is its Muon System [2], conceived to ensure robust, efficient, and redundant detection of muons. The system combines four gas-based technologies — Drift Tubes (DT), Cathode Strip Chambers (CSC), Resistive Plate Chambers (RPC), and Gas Electron Multipliers (GEM) — which together provide precise muon identification, accurate transverse momentum measurements, triggering capabilities, and reliable bunch crossing (BX) assignment. These complementary detectors allow the reconstruction of muons with high efficiency for different physical analyses, from Higgs boson measurements to searches for rare or exotic processes.

2. Resistive Plate Chambers at CMS

Among the technologies implemented in the CMS Muon System, RPCs [1] play a crucial role thanks to their excellent time resolution and fast response. RPCs detect ionizing particles through gas avalanches occurring between resistive electrodes, with the resulting signals collected on readout strips. Their design allows efficient muon triggering and precise bunch crossing identification, ensuring robust performance in the challenging environment of the LHC.

The CMS RPC system covers the pseudorapidity range of $|\eta| < 1.9$ and consists of 1056 chambers: with 480 installed in the barrel and 576 in the endcap regions, totaling over 110,000 electronic readout channels. The chambers employ High Pressure Laminate (HPL) electrodes with bulk resistivity in the range $\rho = 1-6\times10^{10}\Omega\cdot cm$, and operate in avalanche mode using double-gap configurations with 2 mm gas widths. The readout strips have a pitch ranging from 1.74 to 4.1 cm, providing spatial resolutions of about 1 cm, with an average cluster size of roughly two strips [3].

RPCs are required to sustain high particle rates, while maintaining a detection efficiency above 95% and noise rates below 5 Hz/cm^2 [4]. These specifications guarantee the improvement of muon triggering even under high background radiation and over long-term operation, consolidating RPCs as an essential component of the CMS Muon System.

3. Performance at Run 3

During Run 3, the CMS experiment has accumulated an unprecedented amount of data, over 250 fb^{-1} of integrated luminosity. More than 112 fb^{-1} of proton-proton collisions were recorded in 2024, and more than 91 fb^{-1} have been recorded so far in 2025. This large dataset ensures excellent potential for precision measurements and new physics searches, while demanding long-term stability of the subdetectors.

During this period, the performance and stability of the RPC system have been systematically monitored [5] to guarantee the delivery of high-quality data. Continuous validation of detector

PoS(EPS-HEP2025)487

working parameters has confirmed that the RPCs maintain their expected efficiency and low noise operation under the luminosity conditions of Run 3. These results demonstrate the reliability of the RPC system in sustaining optimal performance.

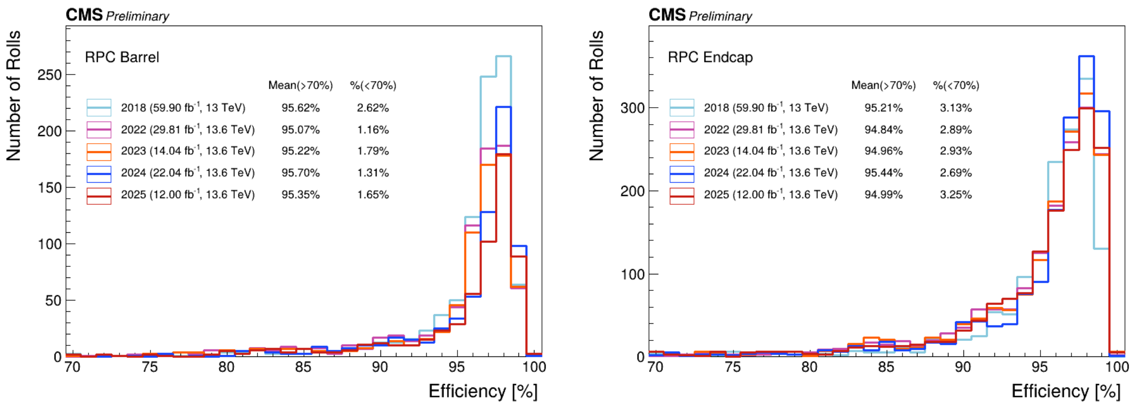

Figure 1: Comparison of RPC overall efficiency distribution in 2018, 2022, 2023, 2024, and 2025. The plots represent the overall efficiency distribution of RPC rolls in Barrel (left) and Endcap (right). Efficiency is obtained using the Segment Extrapolation Method. [8].

The RPC system has demonstrated excellent and stable performance, as illustrated by the overall efficiency distributions shown in Fig. 1. The comparison across multiple years of data taking (2018, 2022, 2023, 2024, and 2025) highlights that the average RPC efficiency remains consistently above 95%, the rolls with known hardware issues or those affected by the CMS gas leak reduction policy are excluded. The detector efficiency is calculated using the Segment Extrapolation method [6].

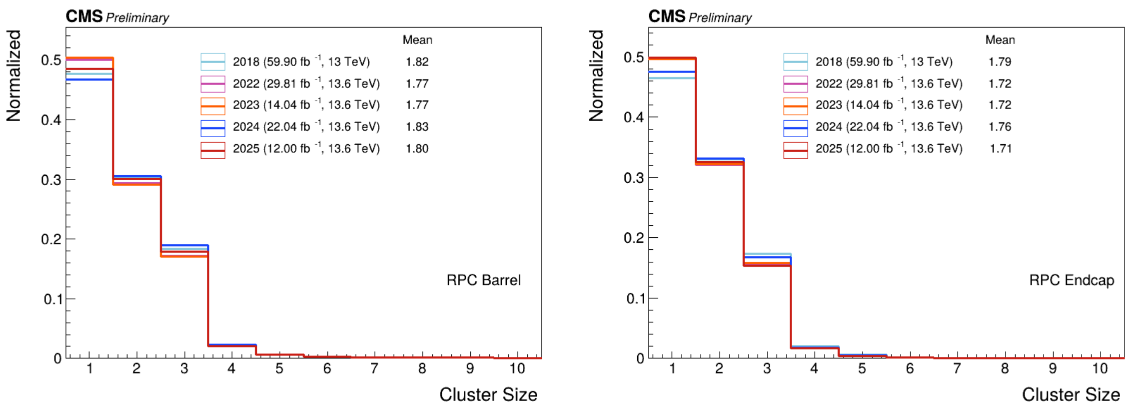

Figure 2: Comparison of RPC cluster size distribution in 2018, 2022, 2023, 2024, and 2025. The plots represent the overall cluster size distribution of RPC rolls in Barrel (left) and Endcap (right). [8].

In addition to efficiency, the RPC cluster size has been monitored. The distributions presented in Fig. 2 show that the average cluster size has remained below two strips in both barrel and endcap regions across all data-taking years, in agreement with design expectations [3].

A detailed view of the RPC performance evolution over time is given in Figs. 3 and 4, which present the efficiency and cluster size history, separately for the barrel and endcap regions. The figures show that the system operated with stable efficiency throughout Run 3, with temporary drops

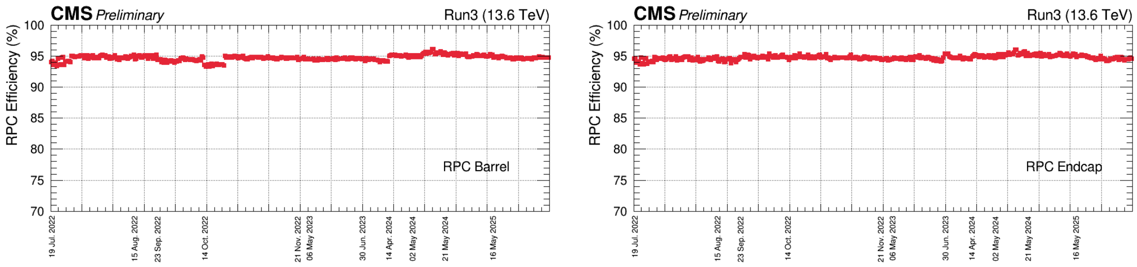

Figure 3: RPC efficiency history vs time for Barrel (left) and Endcap (right). Each point corresponds to an average efficiency in a given CMS run. Data points with low statistics or temporary problems are excluded from the distributions. The detector efficiency is calculated using the Segment Extrapolation method. [8].

clearly correlated with known problematic chambers. In all cases, the issues were either resolved or mitigated through interventions during technical stops, demonstrating the effectiveness of the continuous monitoring and maintenance strategy.

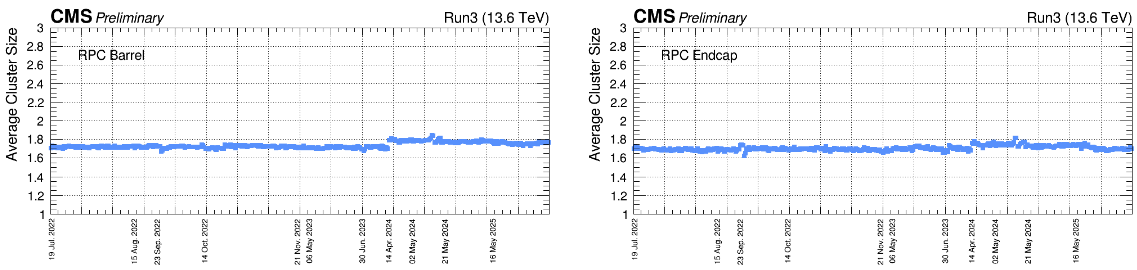

Figure 4: RPC cluster size history vs time for Barrel (left) and Endcap (right). Each point corresponds to an average cluster size in a given CMS run. Data points with low statistics or temporary problems are excluded from the distributions. [8].

4. Working Point Calibration

To guarantee stable operation of the RPC system under varying environmental conditions, the high voltage applied to each detector is carefully calibrated. This procedure, known as the High Voltage (HV) scan, is performed once per year and allows the determination of the optimal operating point, referred to as the Working Point (WP). The HV scan is taken over a series of effective voltages in the range [8600, 9800] V, and the WP for each chamber is defined at 95% of the efficiency curve, plus an additional offset of 100 V for barrel and 120 V for endcap detectors. Small differences between barrel and endcap arise from assembly parameters intrinsic to the detector design. The distributions of RPC efficiency at WP, the WP values themselves, and the average cluster size are shown in Fig. 5.

The analysis of HV scan data has traditionally required manual refinements of the fitting procedure for individual chamber efficiency curves. To improve robustness and reduce the number of failed fits, a machine learning–based algorithm was recently introduced into the calibration workflow [7].

The results, obtained from the most recent HV scans, are consistent with the long-term behavior observed in previous years. Figure 6 summarizes the historical evolution of the RPC working point

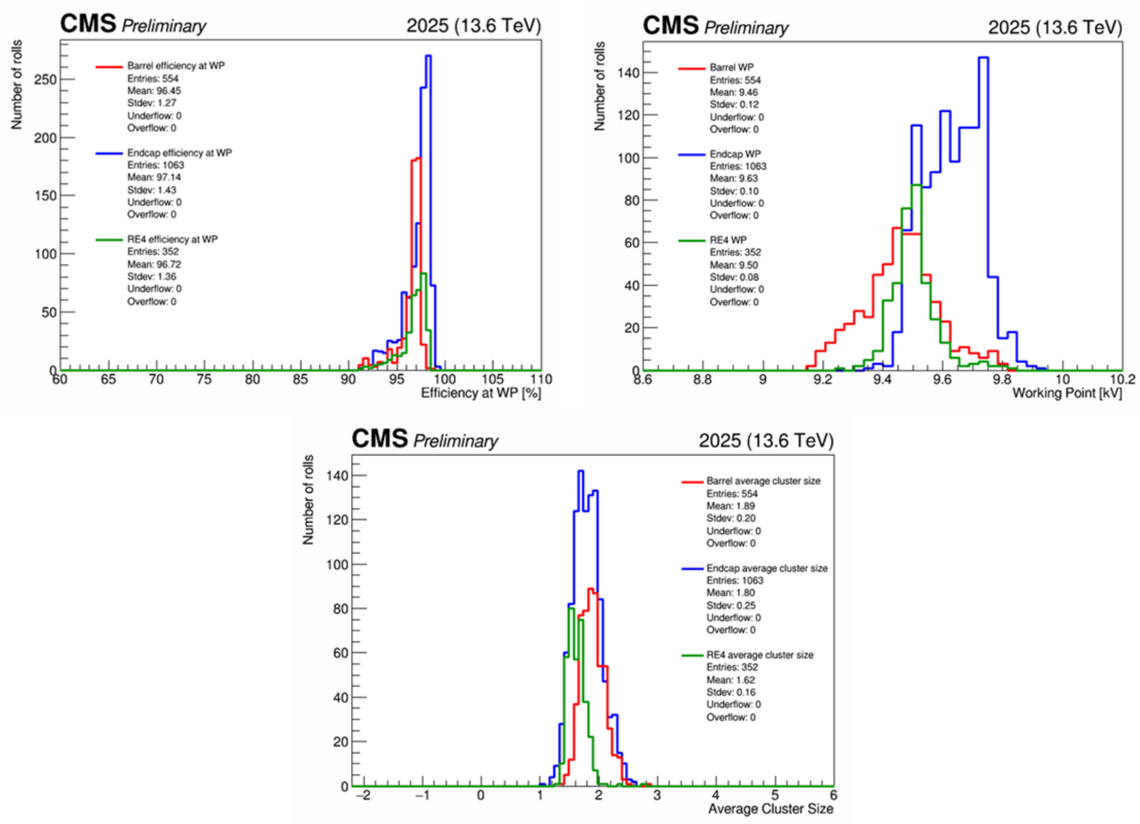

Figure 5: RPC Efficiency at Working Point (top left), Working Point (top right), and Average Cluster Size (bottom) distributions obtained from the HV scan. Data were collected at effective voltages in the range [8600, 9800] V. The red histograms correspond to 554 Barrel rolls, the blue histograms to 1063 Endcap rolls in stations RE1, RE2, and RE3, and the green histograms to 352 rolls in station RE4. [9].

and the efficiency at the working point for the Barrel, Endcap, and RE4 regions. Despite periods without scans during LS1 and LS2, as well as changes in operational conditions over the years, the values of WP and efficiency have remained stable within the expected ranges. This confirms that the detector performance remains well within the optimal operational range.

5. Conclusion

After more than 13 years of operation, the RPC system continues to demonstrate excellent performance. The detectors operate with very high and stable efficiency, consistently above 95%, while maintaining a stable average cluster size of about two strips. In addition, the evolution of the working points has remained remarkably stable throughout the years, confirming both the robustness of the detector design and the effectiveness of the calibration procedures.

6. Acknowledgements

We congratulate our colleagues in the CERN accelerator departments for the excellent performance of the LHC and thank the technical and administrative staffs at CERN and at other CMS

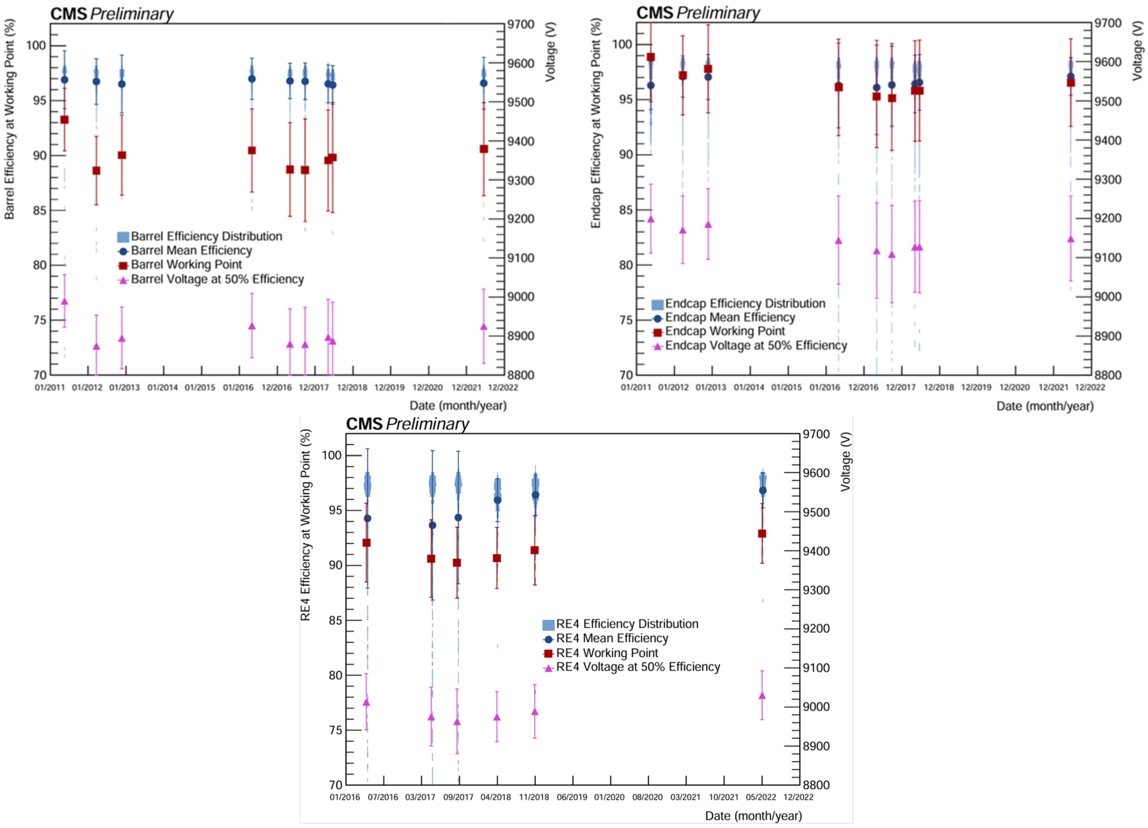

Figure 6: RPC Barrel (top left), Endcap (top right), and Endcap RE4 (bottom) Working Point and Efficiency at Working Point. For this study 9 HV scans taken since 2011 for Barrel and Endcap (RE1, RE2 and RE3) and 6 HV scans taken since 2016 for Endcap RE4 were considered. The working point and the efficiency at the working point evolution is presented. With a blue, full circle is presented the mean efficiency at WP for each of the HV scans. With symmetric light blue bars is presented the efficiency at WP histogram distribution. The magenta, filled triangles indicate the voltage at 50% efficiency. The whiskers (thin, dashed lines) represent the outliers. Red, full squares represent the mean of the working point distribution for each HV scan with their RMS. [10].

institutes for their contributions to the success of the CMS effort. In addition, we gratefully acknowledge the computing centres and personnel of the Worldwide LHC Computing Grid and other centres for delivering so effectively the computing infrastructure essential to our analyses. Finally, we acknowledge the enduring support for the construction and operation of the LHC, the CMS detector, and the supporting computing infrastructure provided by the following funding agencies: FWO (Belgium); CNPq, CAPES and FAPERJ (Brazil); MES and BNSF (Bulgaria); CERN; CAS, MoST, and NSFC (China); MINCIENCIAS (Colombia); CEA and CNRS/IN2P3 (France); SRNSFG (Georgia); IPM (Iran); INFN (Italy); MSIP and NRF (Republic of Korea); BUAP, CINVESTAV, CONACYT, LNS, SEP, and UASLP-FAI (Mexico); PAEC (Pakistan); DOE and NSF (USA).

References

[1] S. Chatrchyan et al. (CMS Collaboration), *The CMS Experiment at the CERN LHC*, JINST **3**, S08004 (2008), doi:10.1088/1748-0221/3/08/S08004.

[2] J. G. Layter (CMS Collaboration), *The CMS Muon Project*, CERN, Geneva, Technical Design Report CMS (1997), `https://cds.cern.ch/record/343814`.

[3] CMS Collaboration, *The Phase-2 Upgrade of the CMS Muon Detectors*, Technical Design Report, CERN-LHCC-2017-012, CMS-TDR-016, CERN, Geneva (2017), doi:10.17181/CERN.5T9S.VPMI, `https://cds.cern.ch/record/2283189`.

[4] CMS Collaboration, *Development of the CMS detector for the CERN LHC Run 3*, JINST 19 (2024) P05064, doi:10.1088/1748-0221/19/05/P05064, `https://iopscience.iop.org/article/10.1088/1748-0221/19/05/P05064`.

[5] M. Shopova et al., *CMS RPC performance and operation in LHC Run 3*, Nuclear Instruments and Methods in Physics Research Section A **1076** (2025) 170467, doi:10.1016/j.nima.2025.170467, `https://www.sciencedirect.com/science/article/pii/S0168900225002682`.

[6] CMS Collaboration, *Performance study of the CMS barrel resistive plate chambers with cosmic rays*, Journal of Instrumentation **5** (2010) T03017, doi:10.1088/1748-0221/5/03/T03017, `https://doi.org/10.1088/1748-0221/5/03/T03017`.

[7] M. Pehlivanova et al., *Machine learning approach to CMS RPC HV scan data analysis*, Nuclear Instruments and Methods in Physics Research Section A **1075** (2025) 170367, doi:10.1016/j.nima.2025.170367, `https://www.sciencedirect.com/science/article/pii/S0168900225001688`.

[8] CMS Collaboration, *RPC Early 2025 Performance*, CMS Detector Performance Summary, CMS-DP-2025/040 (2025), `https://cds.cern.ch/record/2938606`.

[9] CMS Collaboration, *2025 High Voltage Scan Studies for RPC*, CMS Detector Performance Summary, CMS-DP-2025/041 (2025), `https://cds.cern.ch/record/2938607`.

[10] CMS Collaboration, *2022 High Voltage Scan Studies for RPC*, CMS Detector Performance Summary, CMS-DP-2024/105 (2024), `https://cds.cern.ch/record/2916745`.